Real-Time Investigation of Temperature Effect on Induction Motor Equivalent Circuit Parameter Change

Hakan Terzioglu[1, *], Abdullah Cem Agacayak[2]

[1]*Department of Electrical and Electronics Engineering, Faculty of Technology, Selcuk University,
Konya, Turkey*
[2]*Department of Electrical and Energy, Vocational School of Technical Sciences,
Konya Technical University,
Konya, Turkey*
hterzioglu@selcuk.edu.tr

Abstract—Today's developing technology and increasing demands in production areas continue the importance of studies on induction motors (IMs). To meet the demands, the mathematical modeling of IMs must be performed fully and accurately. Variable conditions cause changes in many electrical, magnetic, and thermal parameters. A change in parameters affects the intensity, efficiency of the operating currents of the machine, thereby changing the motor losses.

In this article, the objective is to determine the changes in the equivalent circuit parameters of three-phase squirrel-cage induction motors (SCIMs) with different powers under the variable conditions (stator winding temperature, load, and motor shaft speed). Supervisory control and data acquisition (SCADA) program read real-time information (temperature, current, voltage, power, shaft speed, and torque) from the experiments and necessary calculations were made. When the test results were examined, a maximum of 9 % change was observed in the motor ECPs (R_S, R_2, R_M, X_S, X_2, and X_M) at different shaft speeds as a result of the change in the stator winding temperature between 100 % and 110 %. At different loads, this rate of change increases to 16 %. This has shown that motor shaft speed and load, together with temperature, have a significant effect on the ECPs.

Index Terms—Equivalent electric circuit; Induction motor; Induction motor modeling; Winding temperature estimation.

I. INTRODUCTION

According to the global energy assessment by the International Energy Agency (IAE), electric motor driven systems (EMDSs) are responsible for 53 % of electricity used worldwide [1]. In the EMDS sector, 77 % of the electrical energy consumption is used by mid-size motors with power values below 375 kW. 80 % of the medium size motors used are induction motors (IMs). The large-scale use of IMs makes them ideal candidates for energy efficiency improvements.

Among electric motors, squirrel-cage induction motors (SCIMs) are the most widely used motors in the industry due to their simple and robust structure, low maintenance, low failure rates, low cost, and high efficiency. IMs are

widely preferred motors in industrial applications because their shaft speed changes very little with direct main voltage and under load. Furthermore, the fact that IM shaft speed and position controls can be easily made has made these motors advantageous over other industrial motors in parallel with today's industrial-technological developments.

Today, asynchronous motors, which are widely used in the industrial field, are very important in driving techniques, controllability, efficiency, behavior under all kinds of loads and working conditions. As a result of research and development studies of the factories where IMs are produced, general parameter information is given under constant running temperature and load is as fabrication data. However, in the industrial field, motors must be used in a wide variety of loads and revolutions. Even the running voltage of the same engine and the amount of load on its shaft can differ during or between days. Therefore, temperature changes in the stator winding of the motors created by these variable operating conditions cause the motor parameters to change instantly. This change in the motor parameters causes the motor not to be properly driven and the energy efficiency to be low. The model is used to determine the parameters. Additionally, since the values of each phase are equal in 3-phase motors, it is sufficient to determine the parameters by applying EC on a single phase. Precise knowledge of single-phase EC model parameters of squirrel-cage induction motor is essential for correct sizing of motor electrical protections, operating points and performance estimation, control and diagnostics [2]. Generally, EC parameters are determined by conventional no-load and locked rotor tests (general test methods) [3]. Even today, the fact that the motors and their drivers are designed with the calculations based on the fabrication data of IMs with variable parameters shows that there is still a way to go in the design and control of these motors. Also, above a certain power level, these tests are impractical. Indirect testing is done to overcome these problems. The IEC 60034-2-1 standard provides guidelines for direct and indirect testing based on the determination of motor loss components to extract EC parameters [4]. It is also common

to use simplified equivalent (L-shaped) circuits for parameter estimations. The effect of the amplification factor in the flux-state observer loop made relative to the L-shaped equivalent circuit can be considered for an induction motor equipped with a squirrel-cage rotor. The calculation of the moment by the state observer is based on estimating the stator flux in a fixed coordinate system. It has been found that the accuracy of the state observer performance is better with the increase in the scaling compensation coefficient, but the upper limit of this coefficient is limited by the noise level in the measured variable. The result of the study reveals that modern AC electric drive systems require the development of high-accuracy systems in speed control without the installation of rotor position sensors [5].

When conventional motors with the same power are compared, it is seen that IMs stay longer than other motors with electromagnetic and especially temporary thermal current. Such effects cause some elements of an electrical machine to be at high temperature. High temperature causes a large number of electrical, magnetic, and thermal parameters to change by reducing the torque of the motor. Changes in the parameters affect the intensity of the machine's running currents and thus change the motor losses. However, among the factors that cause changes in the parameters, making parameter estimation based only on the temperature causes the modelling to be incomplete. Therefore, considering the load and the shaft speed of the motor shaft together with the temperature, they appear as an important concept that affects the motor parameters. The fact that an electrical machine performs with high efficiency in the allowable temperature, load, and shaft speed range shows us that the electric machine is well designed. It is of great importance to improve engine performance and reduce cost for both the manufacturer and the user. Since the operating cost constitutes a large part of the total cost, it is of great importance to improve the active materials used in the engine and to correctly determine the engine parameter variables. Continuous measurement of instantaneous parameter changes causes high computer hardware costs during the modelling phase and a very long analysis process. As a result, it is necessary to calculate the parameters of various loads and factors correctly to examine the dynamic performances of the induction motors and to derive their mathematical models. In recent years, the importance of the subject has emerged and number of studies on the determination of electrical equivalent circuit parameters (EECPs) of induction motors have increased. In studies, methods consisting of artificial intelligence techniques are widely used to determine equivalent circuit parameters, which is a nonlinear and multivariate problem. Some of these methods can be listed as genetic algorithms, differential evolution algorithm, particle swarm optimization algorithm, etc.

Although we have mentioned the disadvantages of using only engine manufacturer data for ECP extraction, research using these data continues [6]–[8]. Considering the more complete information provided by the manufacturer, a methodology is presented to obtain the parameters of the equivalent circuit, which has the advantage of allowing the electrical calculation of all power losses and the realization of power balance for medium voltage and high-power induction motors. Three types of losses are considered as part of the balance of power. These are effective conventional or joule variable losses, fixed losses, and additional losses. When a resistor is used in the rotor circuit, additional losses can be calculated [9]. Among the methods proposed in the research, the numerical and analytical dimensionless approach is based on the synergistic interaction using Thevenin's Theorem. Initially, the rated motor parameters and the unknown variables of the equivalent circuit are combined into dimensionless expressions using Thevenin's Theorem [10]. On the contrary, an offline parameterization solution can be made with a particle swarm optimization algorithm to minimize the error between manufacturer data by including precise and deep bar circuit model parameter estimation [11]–[13]. An experimental estimation method has been developed according to the surface effect of rotor current and stator iron loss of the equivalent circuit parameters of the deep bar induction motor. In the method, steady-state currents, stator voltages, and slips are measured at various loads and currents and voltages in the first phase of the motor starting at s = 1. Based on the measurements made using the Fourier transform, the input stator impedances are determined for the slip s = 1 and the slip at various loads. Assuming that the rotor resistances are independent of the surface effect for the working slip values solves the system of nonlinear equations, allowing to find the equivalent current penetration depth to the rotor bar and the parameters of the available surface effect coefficients for the rotor resistance and reactance [14]. A multiobjective genetic algorithm is used, which includes magnetic saturation and surface layer effect on motor magnetization inductance, rotor leakage inductance, and rotor resistance via polynomial functions. With this algorithm, there are also complex EC models where inputs such as input current, torque and slip measurements are obtained [15]. It is also proposed in a differential evolution algorithm-based methodology for an accurate estimation of asynchronous motor ECPs that takes into account temperature, magnetic saturation, and surface layer effect [16]. Finite element analysis (FEA), analytical and numerical approaches are also used to calculate ECPs on over these effects [17]–[20]. In addition, the finite element method (FEM) is another scheme used to determine the increase in temperature in electrical machines and also to analyze the thermal behavior of electrical machines [21]–[23]. However, this analysis method requires a deep knowledge of the geometries and dimensions of the engine. In recent years, evolutionary algorithms have been used successfully to solve this problem. In the past, thermal circuits of induction motors, radial flux [24], fixed axial flux generators [25], and other machines have been studied by proposing a lumped parameter model (LPM) approach. The thermal network model (TNM), which is called the lumped parameter model in the market, is one of the schemes adopted in the study of thermal models for the determination of temperature rise in electrical machines [26], [27]. The lumped parameters are derived entirely from the dimensional information, the thermal properties of the materials used in the design, and the constant temperature

transfer coefficients. This means a high level of adaptability to various sizes of motor body. In addition, calculations of parameter values resulting from lumped editing are relatively complex and result in sets of thermal equations that mathematically fully describe the machine, including motor protection that can be solved and adapted with online temperature monitoring for many applications [28], [29]. The thermal circuit method is used to estimate the increase in temperature of electrical machines using real resistance circuits, in thermal modelling of electrical machines, using numerical methods such as finite element and finite difference analysis [30], [31]. Various studies, including dynamic and thermal modelling of IM have been done for nonlinear effects [32], [33]. Electromechanical or thermal devices are used to protect many motors used in industrial applications from overload. However, thermal overheating and cycling cause accelerated thermal wear, degrading winding insulation. The analysis of the temperature transfer process is usually performed by selecting an idealized machine geometry. Then it is carefully divided into basic elements and is characterized by a node, thermal resistance, thermal capacity, and a temperature source [34]. When describing the basics, much needs to be known about machine construction and the thermal properties of the materials used. To eliminate and reduce this information load, careful division of the machine into several parts gives a better result. However, this introduces great complexity in the computational task. Since this situation causes difficulties in computer simulation and software development, simplified model suggestions are made [35]. Today, general-purpose advanced computational fluid dynamics (CFD) packages are available on the market, which include modern solution methods to improve high-demand thermal modelling of the flow system. These package codes are designed with technology focused on improving the flow system in challenging thermal modelling situations. Electrical machine manufacturers rely on this modelling, especially in the cooling/ventilation modelling [36] and thermal management of alternating current electric motors [37].

When studies on electrical equivalent parameter estimation of IMs, which change with the effect of environmental factors, are evaluated, it does not seem possible to use measurement or equivalent circuit-based methods in motors at the design stage. On the other hand, analytical or FEM-based methods can be used in the design phase. However, it cannot be applied to a pre-manufactured engine. The exact geometry and material data may not always be fully available. An offline parameter estimation can be made using the particle swarm optimization technique. However, this cannot predict online the effects of environmental factors such as temperature and load over time.

Estimates made with only the thermal equivalent parameter are limited and insufficient. In fact, electrical parameters can be approximated using a multiobjective genetic algorithm. However, this method involves complex EC modelling. As a result, it is concluded that the nonlinear and variable parameters of IMs can only be accurately determined by experiments in which multivariate effects are observed together at different motor powers.

In this article, we aim to determine the changes in the ECPs of a three-phase SCIM at different powers under variable conditions (winding temperature, load, and motor shaft speed) during the run. In addition, it is aimed to interpret the parameter test data of our experiments by comparing them with the parameter data obtained by general test methods (idle run and locked rotor tests).

In this study, the environmental conditions that affect the engine parameters were applied to the engines under a single test. In addition, by including the variability of motor power in the experimental content, the effect of the difference in power on the rate of change in the parameters is shown. Thus, our study differs from scientific studies done so far in terms of analyzing so many variables together that have an effect on the parameters. The results of the study, which we obtained by analyzing many environmental effects at the same time, are thought to provide universal modelling in future studies with data mining. When the results of the changes in the ECP to the environmental factors of the IM, whose foundation was laid with this study, are combined with our future studies, it is thought that it will bring a new perspective compared to the studies done so far, both in the driving methods of the IMs and in early failure detection.

II. INDUCTION MOTORS

In 3-phase IMs, the electrical and mechanical properties of each phase are equal. Therefore, when the characteristics of 1-phase in IMs are determined, it means that the ECPs of a 3-phase induction motor are also determined. In other words, when creating an EC in 3-phase IMs, it is sufficient to determine only the 1-phase EC. Figure 1 shows the equivalent circuit of an IM.
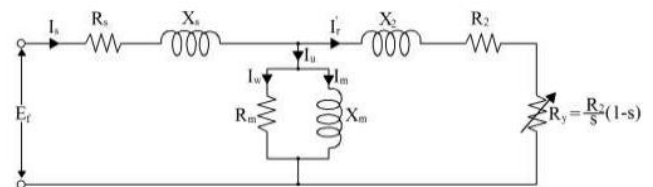

Fig. 1. 1-phase equivalent circuit of an IM.

The parameters of the EC in Fig. 1 are described as follows:

− E_f: A phase voltage value (volt);

− R_s: Internal resistance of the stator winding (Ohm);

− X_s: Leakage reactance of the stator winding (Ohm),

− I_s: Current passing through a stator circuit (Ampere);

− X_2: Equivalent of the leakage reactance of the rotor circuit transferred into the stator circuit (Ohm);

− R_2: Equivalent of rotor circuit resistance transferred to stator circuit (Ohm);

− I_r': Current passing through the rotor circuit (Ampere);

− R_m: Core loss component (Ohm);

− X_m: Magnetizing reactance of the winding (Ohm);

− I_u: Current passing through the excitation circuit (Ampere);

− I_m: Magnetizing current (reactive component of excitation current) (Ampere);

− I_w: The current through resistor R_m (active component of excitation current) (Ampere);

− R_y: Electrical resistance of the load on the motor shaft in stator terms (Ohm).

To simplify the solution in this circuit, a simple equivalent circuit (SEC) is used, which gives results similar to the EC results. In the SEC, R_m, and X_m, which are shunt-connected to the circuit, are shifted in front of the stator winding components R_s and X_s. The SEC is shown in Fig. 2.
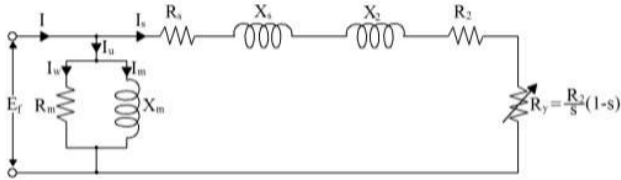

Fig. 2. A simplified 1-phase equivalent circuit of IM.

In the 3-phase IM balance, a simplified 1-phase SEC is designed according to the following conditions:

− The winding resistance of the stator is kept low to reduce the stator copper loss;

− The leakage reactance of the stator winding is minimized by reducing the average wire length of each winding;

− Thin sheets are used to reduce core losses (iron loss). R_m is kept high this way;

− The iron chosen for the plates has high conductivity and the flux density at the operating point of the motor is kept under the lap robe of the magnetization curve. The magnetic reactance is thus high;

− When the exciter shunt connection is brought to the input of the EC, the obtained SEC is given in Fig. 2.

The I symbol is the current drawn by the motor from the mains [38].

III. DESIGN OF TEST

In this study, our objective was to determine the variation of IM electrical magnitudes and EECPs with motor winding temperature. In addition, by interpreting the test data obtained for this purpose, it is requested to compare the general test methods (idle run and Locked Rotor test) with the parameter results. The block diagram of the system test created for the real-time analysis of the variation of parameters with temperature is given in Fig. 3.
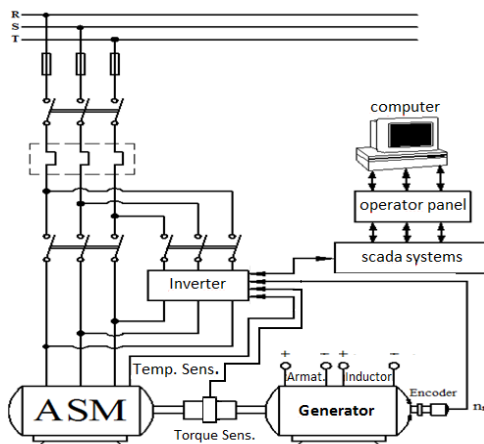

Fig. 3. Experimental block diagram.

In the block diagram in Fig. 3, two different 0.75 kW and 1.5 kW power motors are used as IMs. The dynamo was used to carry out loaded running tests of the IMs. The technical specifications of the IMs and the dynamo used in the tests are given in Table I.

TABLE I. TECHNICAL SPECIFICATIONS OF ASMS.

Tech. Spec.	1. Motor	2. Motor	Genr.
Power (kW)	0.75	1.5	1.5
Voltage (V)	400 - λ	400 - λ	700
Current (A)	1.9	3.6	7.6
Pow. Coefficient	0.75	0.73	-
Frequency (Hz)	50	50	-
Revolution Number (rpm)	1435	1450	3000
Pole Number	4	4	-
Stator Starting resistor (Ω)	20	8.6	-

IM is coupled with Dynamo, Autonics brand 1024 pulse encoder, and DRVL 200 Nm Precision Torque Sensor as shown in Fig. 4. The dynamo DC is fed with a Variac, and the shaft of the IM is loaded.

Fig. 4. Motor-load connection diagram.

The Siemens brand SINAMICS G120 series 5.5 kW driver is used to drive the asynchronous motors. Siemens S7-1200 CPU-1212C 8DI/6DO/2AI programmable logic controller (PLC) and KTP700 Basic PN, 7″ HMI PROFINET interface, 800 × 480 human-machine interface (HMI) display are used for driver control and read data with supervisory control and data acquisition (SCADA) software. The electrical panel with the driver, PLC, and HMI panel is shown in Fig. 5.

Fig. 5. Control unit of induction motor.

The driver was used to read the current, voltage, power factor, power, and torque data of the motors in this investigation. The stator winding temperature information on the motor was received by the PT1000 sensor mounted inside the motor, as shown in Fig. 6.

With the SCADA software on the HMI panel, current, voltage, frequency, power factor, torque, power, shaft speed and temperature data can be accessed in real-time. The changes in the equivalent circuit parameters (R_S, X_S, R_2, X_2, R_M, and X_M) during the experiment can be seen graphically.

An example view of the screen pages containing these data is shown in Fig. 7.

Fig. 6. Placement of the PT1000 temperature sensor on a 0.75 kW motor.
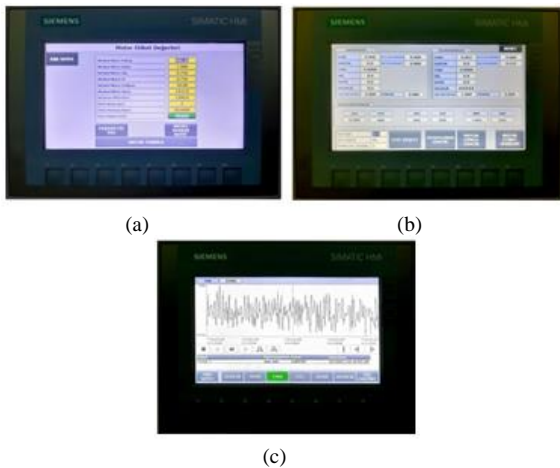

(a)　　　　　　　　　　(b)

(c)

Fig. 7. HMI KTP700 touch screen: a) Instant engine data; b) Engine label data entry page; c) Engine current graphic display pages.

In addition, all the parameters measured and calculated in the system are saved in the memory of the PLC in .Xsl format, and these files can be accessed via the computer. An example experimental setup is shown in Fig. 8.
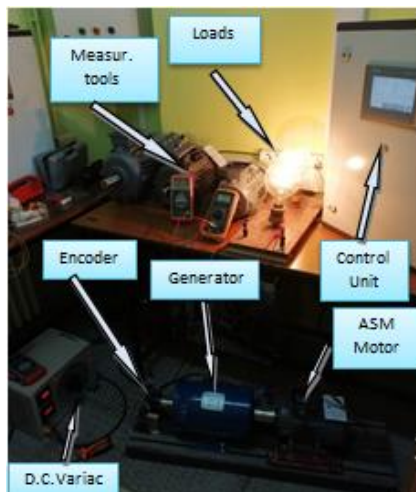

Fig. 8. Experiment connection in loaded operation.

Motors with different powers (0.75 kW–1.5 kW) were connected to their shafts with a compound DC generator with the help of a coupling, and a regulated load (25 %-50 %-75 % and 100 %) was loaded onto the motor by giving DC energy to the externally adjusted Variac windings. With the compound generator, IM's were loaded

with the most ohmic load they have ever encountered in the industry.

IV. RESULTS FROM THE TESTS

The tests were carried out at two different engine powers (0.75 kW–1.5 kW), at no load, at two different loads (50 % and 100 %), and at two different shaft speeds (750 and 1500). At the beginning of the test, the values on the motor label (Nominal motor voltage, Nominal motor current, Nominal motor power factor, Maximum motor speed and motor pole number) and motor stator winding resistance were entered into the SCADA system. The values of the output parameters (R_S, X_S, R_2, X_2, R_M, and X_M) were calculated according to the input parameters (voltage, current, torque, power, power factor, frequency, and stator winding temperature) measured during the test.

If the motor is star connected, a DC resistance (R_{dc}) will be obtained when measured between the two phase terminals (U, V). As seen in Fig. 9, this measured R_{dc} is the total resistance of the two windings. The resistance of one phase winding of the motor is calculated as
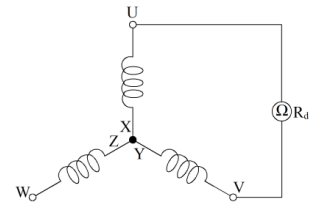
$$R = \frac{R_{dc}}{2}. \tag{1}$$

Fig. 9. Measurement of the stator resistance of a star connected induction motor with an ohmmeter.

Since the motor operates in alternating current, to calculate the effective resistance of the stator windings (alternating current ohmic resistance), it is necessary to multiply the ohmic resistance measured in direct current from 1.2 to 1.5 times

$$R_s = R (1.2 - 1.5). \tag{2}$$

If the motor is connected in delta as in Fig. 10, the measured direct current resistance (R_{dc}) between the stator winding ends:

$$R = \frac{3 R_{dc}}{2} = 1.5 R_{dc}, \tag{3}$$

$$R_s = 1.5 R (1.2 - 1.5), \tag{4}$$

$$R_{sy} = R_s [1+\alpha(t_2 - t_1)], \tag{5}$$

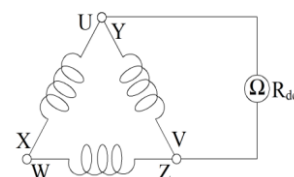where $\alpha = 0.0039$ (temperature coefficient of copper).

Fig. 10. Measurement of the stator resistance of a delta-connected induction motor with an ohmmeter.

IM slip:

$$s = \frac{n_s - n_r}{n_s} = \frac{\omega_s - \omega_r}{\omega_s}, \qquad (6)$$

$$\omega_s = \frac{n_s \pi}{180}, \qquad (7)$$

$$n_s = \frac{120 f}{2\pi}, \qquad (8)$$

$$T_m = \frac{3}{\omega_s} \frac{R_2}{s} I_s^2, \qquad (9)$$

$$I_1 = \frac{U_1}{\sqrt{(R_1 + R_2)^2 + (X_1 + X_2)^2}}, \qquad (10)$$

$$R_2 = \frac{T_m \omega_s s}{3 I_s^2}, \qquad (11)$$

$$R_{2y} = \left(\frac{P_s}{3 I_s^2} - R_{sy} \right) s = \frac{P_m s}{3(1-s) I_s^2} =$$

$$= \frac{T_m \omega_r s}{3(1-s) I_s^2}, \qquad (12)$$

$$R_e = R_s + R_{2y}, \qquad (13)$$

$$X_e = \sqrt{\frac{V_s^2}{I_s^2} - R_e}, \qquad (14)$$

$$X_s = X_2 = \frac{X_e}{2}. \qquad (15)$$

From the approximate equivalent circuit (P_0 = Idle Power),

$$P_0 = \sum P_{fe}, \qquad (16)$$

$$\frac{P_0}{3} = \frac{V_1^2}{R_m} \Rightarrow R_m = \frac{3 V_1^2}{P_0}, \qquad (17)$$

$$I_w = \frac{V_1}{R_m}, \qquad (18)$$

$$I_0 = \frac{I_1}{\sqrt{3}}, \qquad (19)$$

$$I_0 = \sqrt{I_w^2 + I_m^2} \Rightarrow I_m =$$

$$= \sqrt{I_w^2 - I_0^2}, \qquad (20)$$

$$X_m = \frac{V_1}{I_m}. \qquad (21)$$

The variation of each test input and output parameters was tested with temperature. To visualize the data in a more understandable way, its graphical variations (Fig. 11) are given. In the graphs in the figure, the letter (Y) is seen next to some parameters. These parametric symbols are used instead of the approximate equivalent circuit parameter. For example, it is symbolized as X_{SY} instead of X_s'. The change of other data will be analyzed in the form of a data table.

When the graphics were examined, the no-load test parameters of the 0.75 kW and 1.5 kW motors showed more oscillation than the loaded test parameters. These oscillations decrease when the motors are loaded. This is due to the oscillation in the current. The graphs in the figure are drawn by averaging the values read in real-time according to the determined sampling time. The blue line on the graph shows the parameter change per second, while the black line on the graph shows the average of the parameter oscillation values.

Since it is important to correctly determine electrical parameters in IMs, the input parameters were calculated with traditional formulas according to the output parameters of the system obtained in the tests. Thus, it was possible to compare both the input parameters received from the system and the calculated input parameters. The compatibility of the system and software installed as a result of the comparison has been verified. The recalculation of the output parameters according to the input parameters obtained from the test setup is given in Table II.

Since the main purpose of our study was to change the parameters according to the stator winding temperature, the values were taken at the start and end temperatures of these general tests. The input parameters (voltage, current, power, and stator winding resistance) obtained from these tests are shown in Table III. During motor operation, oscillations occur in the current. Since it is averaged and written in the table, it is expressed as the current symbol (Iavg.).

We cannot obtain the stator winding temperature changes during a motor run-time in parameter determination with general test methods. Therefore, in the general test method tests (idle and locked rotor), the parameter values at the motor stator winding temperature at the start of the test and the motor stator winding temperature at the end of the determined test period were determined. The parameter values determined and the output parameters obtained from the system test performed with the software are compared in Table IV.

When Table IV was examined, the error rates were found to be very low between the parameters determined in the system test and the parameters determined by general tests. Furthermore, the parameters in all the tests appear to change by 10 % or less under the influence of temperature.

The effect of the motor stator winding temperature on the parameters calculated from the general tests and the parameters obtained from the system test was plotted graphically. When the graphs are examined, the variation of both experimental parameters with temperature shows parallelism. Figure 12 shows graphs of these rates of change.

As can be seen from the graph, the change rates of the parameters obtained as a result of the calculations made in the system test and general tests are very close and compatible.

It was mentioned that changes in the parameters during the motor run-time will not only depend on the winding temperature of the stator. It is known that, in addition to the temperature effect, it is a factor in the motor shaft speed and load.

In Fig. 13, the effects of 0.75 kW and 1.5 kW motor shaft speed and stator winding temperature on the parameter are compared in the no-load and loaded run tests.
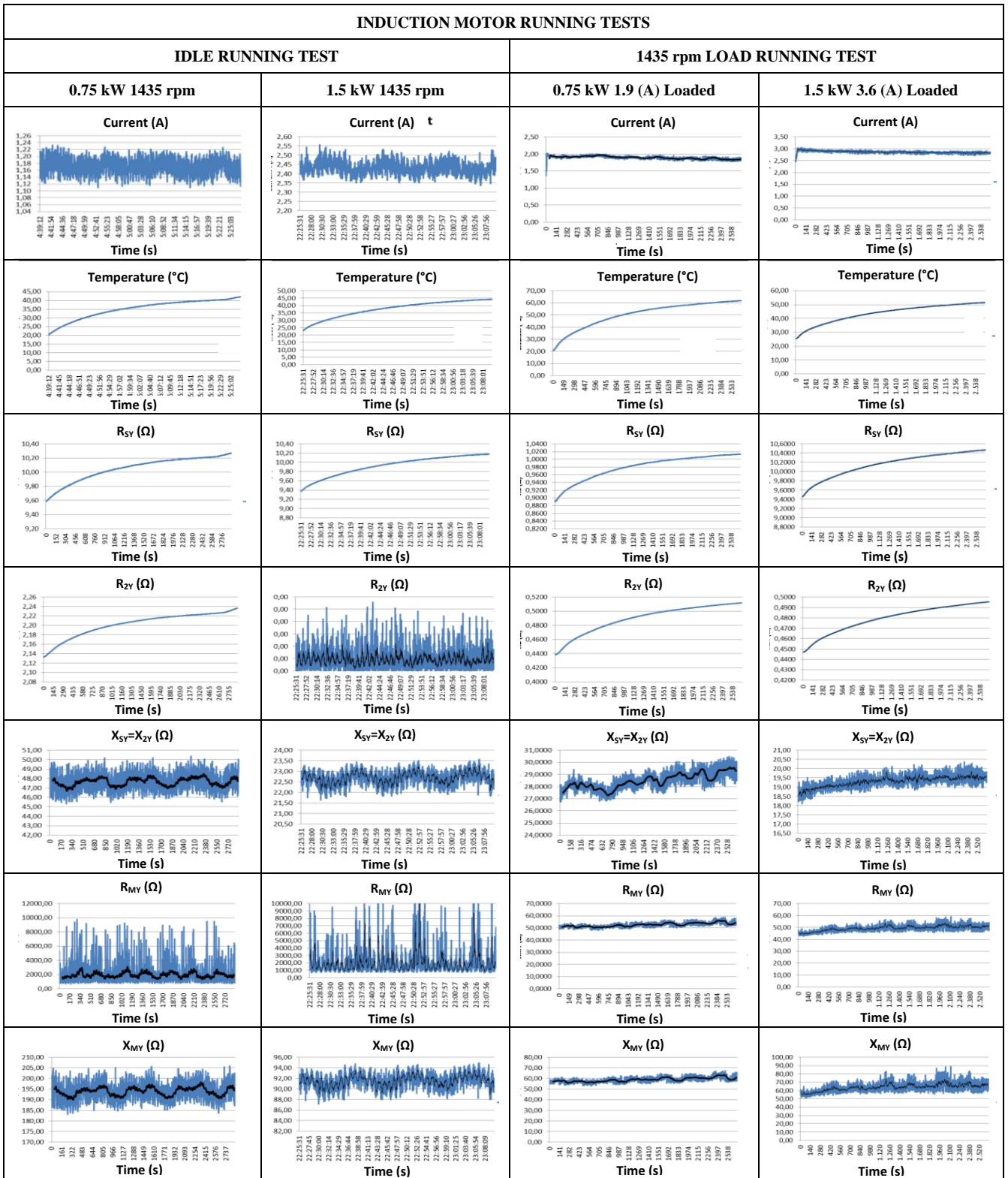
Fig. 11. Induction motor running test graphics.

TABLE II. COMPARISON OF CALCULATED DATA WITH ASYNCHRONOUS MOTOR LOAD TEST DATA.

P (kW)	n (rpm)	LOAD %		ELECTRICAL DIMENSIONS									
				Meas. Voltage (V)	Meas. Current (A)	Calc. Current (A)	Current (%)	Meas. Power (W)	Calc. Power (W)	Power (%)	Meas. Torque	Calc. Torque	Torque (%)
0.75	375	25	Initial Value	105.59	1.31	1.26	3.55	68.30	70.82	3.69	1.77	1.74	3.69
			Average Value	105.87	1.33	1.26	4.90	172.08	177.00	2.86	4.38	4.38	2.86
0.75	750	50	Initial Value	206.35	1.33	1.33	0.20	52.11	54.55	4.68	0.66	0.66	4.68
			Average Value	206.79	1.51	1.46	3.46	309.19	308.96	0.08	3.94	3.94	0.08

P (kW)	n (rpm)	LOAD %		ELECTRICAL DIMENSIONS									
				Meas.	Meas.	Calc.		Meas.	Calc.		Meas.	Calc.	
				Voltage (V)	Current (A)	Current (A)	Current (%)	Power (W)	Power (W)	Power (%)	Torque	Torque	Torque (%)
0.75	1125	75	Initial Value	301.84	1.74	1.81	4.01	167.43	171.19	2.25	1.42	1.42	2.25
			Average Value	302.00	1.70	1.68	0.93	663.98	672.46	1.28	5.64	5.64	1.28
0.75	1500	100	Initial Value	109.55	1.42	1.40	1.31	31.26	32.72	4.68	0.80	0.80	4.68
			Average Value	110.13	1.40	1.36	3.06	134.53	129.95	3.41	3.43	3.43	3.41
1.5	375	50	Initial Value	107.13	2.86	2.92	2.01	100.07	102.92	2.85	2.55	2.55	2.85
			Average Value	107.53	2.83	2.78	1.59	91.61	95.34	4.07	2.33	2.33	4.07
1.5	750	25	Initial Value	204.59	2.75	2.80	1.85	47.12	49.44	4.93	0.69	0.66	4.93
			Average Value	204.84	2.77	2.73	1.57	46.45	48.64	4.73	0.60	0.59	4.73
1.5	1125	100	Initial Value	301.85	2.71	2.69	0.47	154.14	160.80	4.32	1.31	1.31	4.32
			Average Value	301.96	2.90	2.78	4.16	767.32	791.68	3.17	6.51	6.52	3.17
1.5	1500	75	Initial Value	390.88	2.44	2.60	6.35	223.13	232.31	4.11	1.42	1.42	4.11
			Average Value	399.99	2.74	2.84	3.74	736.95	734.14	0.38	4.69	4.69	0.38

TABLE III. INDUCTION MOTOR IDLING AND LOCKED ROTOR TEST DATA.

	0.75 kW λ					1.5 kW λ			
	Idle Running	Locked Rotor	Idle Running	Locked Rotor		Idle Running	Locked Rotor	Idle Running	Locked Rotor
	Temperature 20.35 °C		Temperature 42.20 °C			Temperature 22.91 °C		Temperature 44.11 °C	
Power Value (W)	330	326	353.66	315.76	Power Value (W)	789.60	396.60	879	402.80
Iavg. (A)	0.98	1.21	1.17	1.38	Iavg. (A)	2.09	2.68	2.13	2.59
Voltage Value (V)	221.60	31.25	224.63	31.95	VoltageValue (V)	221.60	31.95	224.63	32.25

TABLE IV. INDUCTION MOTOR IDLING AND LOCKED ROTOR TEST DATA.

0.75 kW/λ									Percentage Changes in Parameters with Temperature in Idle/Locked Rotor Test (%)	Percentage Changes in Parameters with Temperature in System Test (%)
	Idle Running	Locked Rotor	Test Parm.	Error Rate	Idle Running	Locked Rotor	Test Parm.	Error Rate		
	Temperature 20.35 °C				Temperature 42.20 °C				107.37	
R_S (Ω)	14.07	14.34	1.95		14.98	15.28	2.00		6.47	6.52
R_2 (Ω)	209.21	213.24	1.93		151.31	150.52	0.52		27.68	29.41
R_M (Ω)	148.81	148.10	0.48		142.68	142.68	0.00		4.12	3.66
X_S (Ω)	49.10	48.55	1.12		48.31	47.99	0.66		1.61	1.16
X_2 (Ω)	49.10	48.55	1.12		48.31	47.99	0.66		1.61	1.16
X_M (Ω)	198.31	197.69	0.31		213.90	211.85	0.96		7.86	7.17

| 1.5 kW/λ									Percentage Changes in Parameters with Temperature in Idle/Locked Rotor Test (%)	Percentage Changes in Parameters with Temperature in System Test (%)
	Idle Running	Locked Rotor	Test Parm.	Error Rate	Idle Running	Locked Rotor	Test Parm.	Error Rate		
	Temperature 22.91° C				Temperature 44.11 °C				92.54	
R_S (Ω)	6.02	6.05	0.53		6.44	6.44	0.07		6.98	6.50
R_2 (Ω)	49.28	48.83	0.92		53.85	53.56	0.54		9.28	9.69
R_M (Ω)	62.19	62.90	1.14		57.40	58.31	1.58		7.70	7.29
X_S (Ω)	27.19	27.14	0.21		29.73	24.79	16.62		9.32	8.66
X_2 (Ω)	27.19	27.14	0.21		29.73	24.79	16.62		9.32	8.66
X_M (Ω)	76.79	75.76	1.34		68.47	67.94	0.76		10.84	10.31
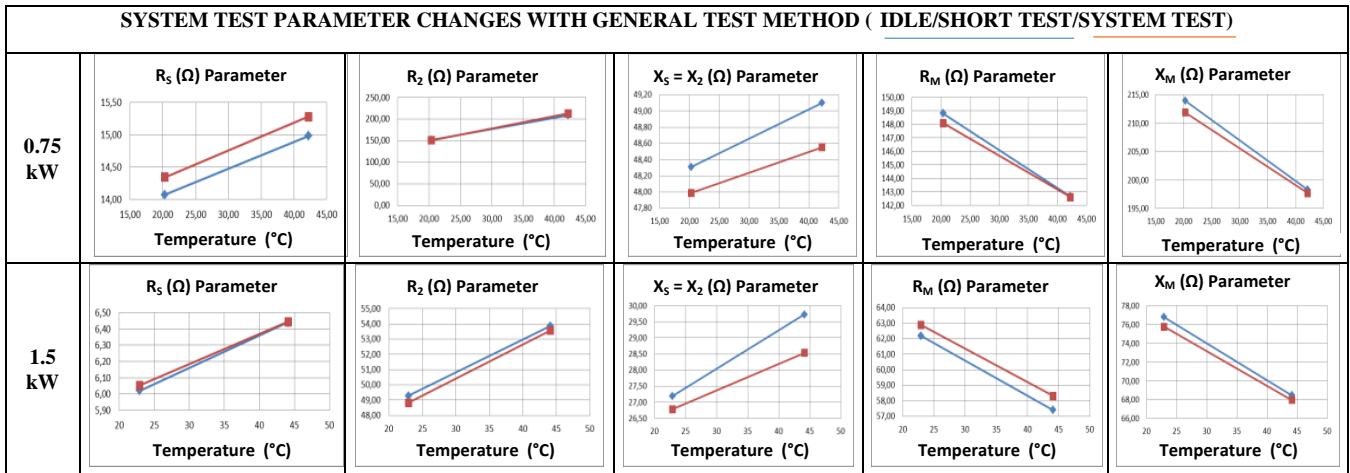
Fig. 12. Graphical comparison of induction motor idle/locked rotor test data and system test data.
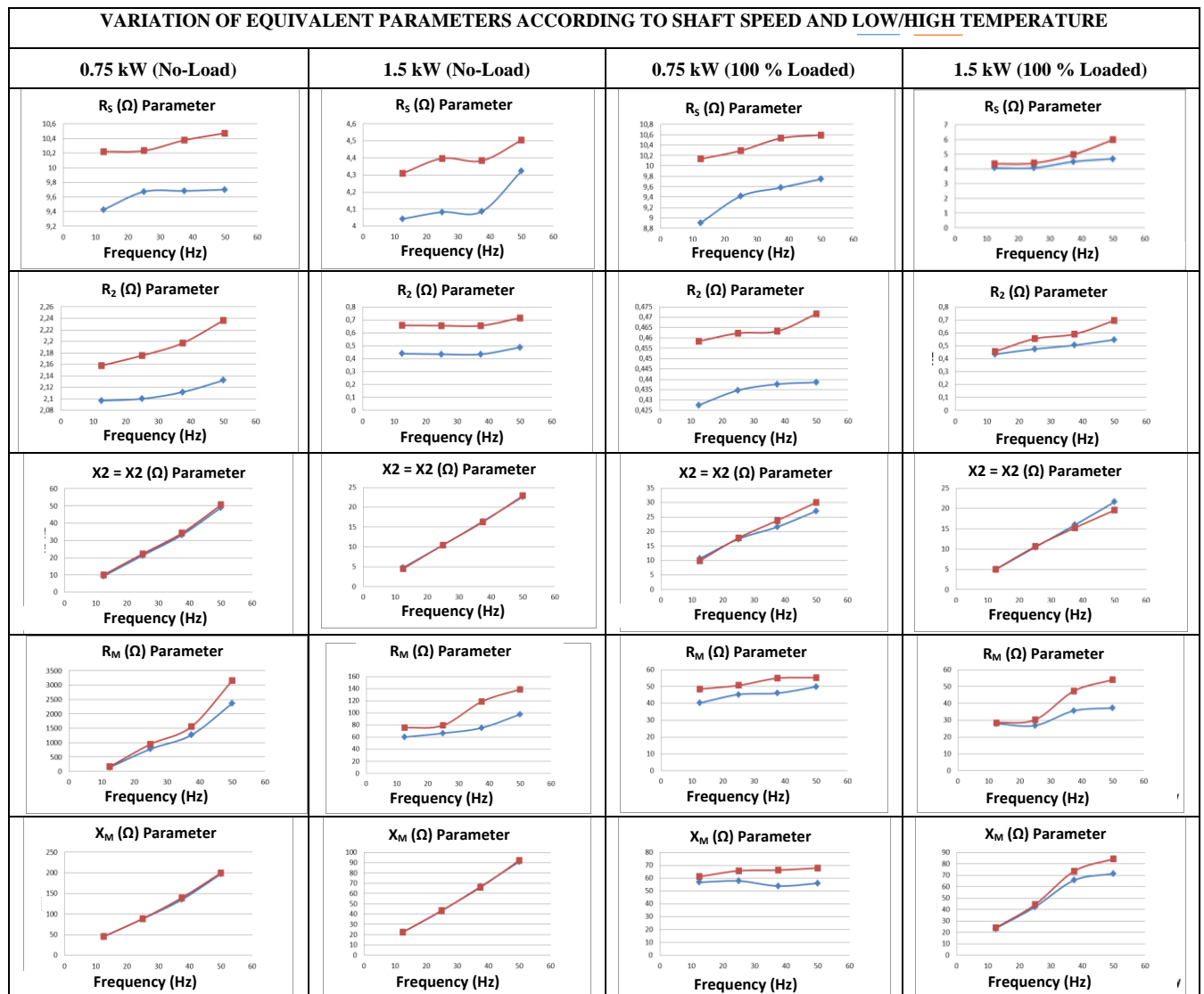

Fig. 13. Variations in the idle/loaded parameters of the induction motor depending on frequency and temperature.

V. DISCUSSION

The statistical analysis presented in the test results section allowed us to reach the following conclusions:

1. The parameters of asynchronous motors vary by about 10 % according to motor power and environmental factors (stator winding temperature, load, and spindle speed);

2. The error rate mostly below 1 % between the data of the proposed method and the general asynchronous motor test data indicates the reliability of the system;

3. The highest oscillation values in the parameters occurred in the no-load tests. The motors work more stable under load and the parameters show less oscillation;

4. The parameter change curves determined by various calculation methods in all engine operating conditions are very close to each other.

This article partially determined the effect of temperature change in IM windings on motor parameters in a preliminary study. In our future studies, the scope of the change in the IM parameters will be expanded to include different IM powers, different speeds and different loads, and temperature transfer losses will be analyzed. Thus, an accurate thermal model for the IM will be developed. When creating this model, it is aimed to present mathematical modelling by processing many data stacks showing the electrical equivalent parameters. The mathematical modelling, which we aim to find, will cover not only the engines in the design phase, but also the engines that have been manufactured before. In addition, it is thought that universal modelling will be presented by analyzing many environmental effects at the same time. This modelling will be a mathematical modelling that is simple to use and we can get results quickly. Thus, it is thought that the mathematical modelling that we obtained as a result of our research will bring a new perspective to both the driving methods of IMs and early failure detection compared to the studies done so far.

VI. CONCLUSIONS

In this study, the parameter determination of the IMs was done with the experimental setup consisting of the SCADA system. At the beginning of the test, the motor manufacturer's data were combined with the input parameters measured by the driver, and the output parameters of three-phase SCIMs with two different powers (0.75 kW and 1.5 kW) were determined. In the experiments, the effects of environmental factors (stator winding temperature, shaft speed, and load) on the motor equivalent circuit parameters were determined.

Variables of parameters determined by environmental factors are also presented graphically in the article. In addition, the parameters of these engines were calculated by general tests. The general test parameters were compared with the parameters measured and calculated by the designed system. With this comparison, the accuracy of parameter determination in the designed system is shown, and how it changes with environmental factors is presented graphically.

From the test results we obtained, the ECPs of IMs are affected at different rates according to the types of environmental factors. In this study, the inadequacy of mathematical modelling based on a single environmental factor has been revealed in the light of the data. Although the variability of the parameters is mostly in the winding temperature, we can see from the graphs that it has an effect on the speed and the load on the rotor shaft. For universal mathematical modelling in IM parameter determination, the study has proven that we need to consider the whole environment together. The results of our study are believed to lead to future studies.

REFERENCES

[1] *IEC 60034-2-1 Rotating electrical machines - Part 2-1: Standard methods for determining losses and efficiency from tests (excluding machines for traction vehicles)*, International Standard, International Electrotechnical Commission, Jun. 2014.

[2] H. A. Toliyat, E. Levi, and M. Raina, "A review of RFO induction motor parameter estimation techniques", *IEEE Transactions on Energy Conversion*, vol. 18, no. 2, pp. 271–283, 2003. DOI: 10.1109/TEC.2003.811719.

[3] R. Krishnan, *Electric Motor Drives: Modeling, Analysis, and Control*. Upper Saddle River: Prentice Hall, 2001.

[4] D. G. Dorrell, "A review of the methods for improving the efficiency of drive motors to meet IE4 efficiency standards", *Journal of Power Electronics*, vol. 14, no. 5, pp. 842–851, 2014. DOI: 10.6113/JPE.2014.14.5.842.

[5] A. Ozdil, Y. Uzun, "Design and Analysis of a Rotor for a 22 kW Transversally Laminated Anisotropic Synchronous Reluctance Motor", *Elektron Elektrotech*, vol. 27, no. 6, pp. 17–24, 2021. DOI: 10.5755/j02.eie.29046.

[6] M. Gomez-Gonzalez, F. Jurado, and I. Pérez, "Shuffled frog-leaping algorithm for parameter estimation of a double-cage asynchronous machine", *IET Electric Power Applications*, vol. 6, no. 8, pp. 484–490, 2012. DOI: 10.1049/iet-epa.2011.0262.

[7] M. I. Mossad, M. Azab, and A. Abu-Siada, "A novel evolutionary technique to estimate induction machine parameters from name plate data", in *Proc. of 2016 XXII International Conference on Electrical Machines (ICEM)*, 2016, pp. 66–71. DOI: 10.1109/ICELMACH.2016.7732507.

[8] C. A. C. Wengerkievicz *et al.*, "Estimation of three-phase induction motor equivalent circuit parameters from manufacturer catalog data", *Journal of Microwaves, Optoelectronics and Electromagnetic Applications*, vol. 16, no. 1, pp. 90–107, 2017. DOI: 10.1590/2179-10742017v16i1873.

[9] L. Collazo Solar, A. A. Costa Montiel, M. Vilaragut Llanes, V. Sousa Santos, and A. Curbelo Colina, "A new exact equivalent circuit of the medium voltage three-phase induction motor", *International Journal of Electrical and Computer Engineering (IJECE)*, 2020. DOI: 10.11591/ijece.v10i6.pp6164-6171.

[10] S. Rajput, E. Bender, and M. Averbukh, "Simplified algorithm for assessment equivalent circuit parameters of induction motors", *IET Electric Power Applications*, vol. 14, no. 3, pp. 426–432, 2020. DOI: 10.1049/iet-epa.2019.0822.

[11] V. P. Sakthivel, R. Bhuvaneswari, and S. Subramanian, "Multi-objective parameter estimation of induction motor using particle swarm optimization", *Engineering Applications of Artificial Intelligence*, vol. 23, no. 3, pp. 302–312, 2010. DOI: 10.1016/j.engappai.2009.06.004.

[12] G. F. V. Amaral, J. M. R. Baccarini, F. C. R. Coelho, and L. M. Rabelo, "A high precision method for induction machine parameters estimation from manufacturer data", *IEEE Transactions on Energy Conversion*, vol. 36, no. 2, pp. 1226–1233, 2021. DOI: 10.1109/TEC.2020.3032320.

[13] H. Gorginpour, "Analytical calculation of the equivalent circuit parameters of non-salient pole large synchronous generators", *Journal of Operation and Automation in Power Engineering*, vol. 9, no. 2, pp. 172–181, 2021. DOI: 10.22098/JOAPE.2021.8397.1582.

[14] V. F. Syvokobylenko and S. N. Tkachenko, "Experimental estimation of equivalent circuit parameters of a deep bar induction motor", in *Proc. of 2020 XI International Conference on Electrical Power Drive Systems (ICEPDS)*, 2020, pp. 1–6. DOI: 10.1109/ICEPDS47235.2020.9249326.

[15] P. Kumar, A. Dalal, and A. K. Singh, "Identification of three phase induction machines equivalent circuits parameters using multi-objective genetic algorithms", in *Proc. of 2014 International Conference on Electrical Machines (ICEM)*, 2014, pp. 1211–1217. DOI: 10.1109/ICELMACH.2014.6960336.

[16] A. M. Silva, J. Alberto, C. H. Antunes, and F. J. Ferreira, "A stochastic optimization approach to the estimation of squirrel-cage induction motor equivalent circuit parameters", in *Proc. of 2020 International Conference on Electrical Machines (ICEM)*, 2020, pp.

45–51, vol. 1. DOI: 10.1109/ICEM49940.2020.9270775.

[17] Z. Ling, L. Zhou, S. Guo, and Y. Zhang, "Equivalent circuit parameters calculation of induction motor by finite element analysis", *IEEE Transactions on Magnetics*, vol. 50, no. 2, pp. 833–836, art. no. 7020604, 2014. DOI: 10.1109/TMAG.2013.2282185.

[18] A. Boglietti, A. Cavagnino, L. Ferraris, and M. Lazzari, "Skin effect experimental validations of induction motor squirrel cage parameters", in *Proc. of 2008 18th International Conference on Electrical Machines*, 2008, pp. 1–4. DOI: 10.1109/ICELMACH.2008.4799971.

[19] I. Boldea and S. A. Nasar, *The Induction Machines Design Handbook*, 2nd ed., CRC Press, 2009. DOI: 10.1201/9781315222592.

[20] E. B. Agamloh, A. Cavagnino, and S. Vaschetto, "Accurate determination of induction machine torque and current versus speed characteristics", *IEEE Transactions on Industry Applications*, vol. 53, no. 4, pp. 3285–3294, 2017. DOI: 10.1109/TIA.2017.2675984.

[21] M. R. Feyzi and A. M. Parker, "Heating in deep-bar rotor cages", *IEEE Proceedings - Electrical Power Applications*, vol. 144, no. 4, pp. 271–276, 1997. DOI: 10.1049/ip-epa:19971055.

[22] J. P. Bastos, M. F. Cabreira, N. Sadowski, and S. R. Aruda, "A thermal analysis of induction motors using a weak coupled modeling", *IEEE Transactions on Magnetics*, vol. 33, no. 2, pp. 1714–1717, 1997. DOI: 10.1109/20.582603.

[23] A. Cassat, C. Espanet, and N. Wavre, "BLDC motor stator and rotor iron losses and thermal behaviour based on lumped schemes and 3-D FEM analysis", *IEEE Transactions on Industry Applications*, vol. 39, no. 5, pp. 1314–1322, 2003. DOI: 10.1109/TIA.2003.816480.

[24] Z. J. Liu, D. Howe, P. H. Mellor, and M. K. Jenkins, "Thermal analysis of permanent magnet machines", in *Proc. of 1993 Sixth International Conference on Electrical Machines and Drives (Conf. Publ. No. 376)*, 1993, pp. 359–364.

[25] Z. W. Vilar, D. Patterson, and R. A. Dougal, "Thermal analysis of a single-sided axial flux permanent magnet motor", in *Proc. of 31st Annual Conference of IEEE Industrial Electronics Society, 2005*, 2005, p. 5. DOI: 10.1109/IECON.2005.1569311.

[26] O. S. Ejiofor, A. Chukwemeka, C. Nnonyelu, and O. I. Okoro, "Thermal modelling and analysis of a 10hp induction machine using the lumped parameter approach", *International Journal of Integrated Engineering*, vol. 13, no. 6, pp. 166–179, 2021. DOI: 10.30880/ijie.2021.13.06.016.

[27] P. H. Mellor, D. Roberts, and D. R. Turner, "Lumped parameter model for electrical machines of TEFC design", *IEE Proceedings B Electric Power Applications*, vol. 138, no. 5, pp. 205–218, 1991. DOI: 10.1049/ip-b.1991.0025.

[28] P. H. Mellor, D. Roberts, and D. R. Turner, "Microprocessor based induction motor thermal protection", in *Proc. of 2nd International Conference on Electrical Machines, Design and Applications*, 1985, pp. 16–20.

[29] P. H. Mellor and D. R. Turner, "Real time prediction of temperatures in an induction motor using a microprocessor", *Electric Machines and Power Systems*, vol. 15, nos. 4–5, pp. 333–352, 1988. DOI: 10.1080/07313568808909342.

[30] J. Saari, "Thermal modelling of high-speed induction machines", in *Acta Polytechnica Scandinavica. Electrical Engineering Series No. 90*. Finnish Academy of Technology, 1998.

[31] C. R. Soderberg, "Steady flow of heat in large turbine-generators", *Transactions of the American Institute of Electrical Engineers*, vol. 50, no. 2, pp. 782–798, 1931. DOI: 10.1109/T-AIEE.1931.5055870.

[32] O. S. Ejiofor, O. I. Okoro, and Nwangwu E.O, "A review of the application of lumped parameters and finite element methods in the thermal analysis of electric machines", in *Proc. of ESPTAE 2008, National Conference*, 2008, pp. 149–159, vol. 143.

[33] O. I. Okoro and E. Chikuni, "Electrical and thermal analysis of asynchronous machine for wind energy generation", *International Journal of Sustainable Energy*, vol. 27, no. 1, pp. 1–13, 2008. DOI: 10.1080/14786450802042828.

[34] S.-B. Lee, T. G. Habetler, R. G. Harley, and D. J. Gritter, "An evaluation of model-based stator resistance estimation for induction motor stator winding temperature monitoring", *IEEE Transactions on Energy Conversion*, vol. 17, no. 1, pp. 7–15, 2002. DOI: 10.1109/60.986431.

[35] P. C. Krause and C. H. Thomas, "Simulation of symmetrical induction machinery", *IEEE Transactions on Power Apparatus and Systems*, vol. 84, no. 11, pp. 1038–1053, 1965. DOI: 10.1109/TPAS.1965.4766135.

[36] S. J. Pickering, D. Lampard, and M. Shanel, "Modelling ventilation and cooling of rotors of salient pole machines", in *Proc. of IEMDC 2001. IEEE International Electric Machines and Drives Conference (Cat. No.01EX485)*, 2001, pp. 806–808, 2001. DOI: 10.1109/IEMDC.2001.939411.

[37] C. Liao, C.-L. Chen, and T. Katcher, "Thermal management of AC induction motors using computational fluid dynamic modelling", in *Proc. of IEEE International Electric Machines and Drives Conference. IEMDC'99. Proceedings (Cat. No.99EX272)*, 1999, pp. 189–191. DOI: 10.1109/IEMDC.1999.769067.

[38] M. Selek and H. Terzioğlu, "Determination of equivalent circuit parameters of induction motors by using heuristic algorithms", *Selcuk University Journal of Engineering, Science and Technology*, vol. 5, no. 2, pp. 170–182, Jun. 2017. DOI: 10.15317/Scitech.2017.80.